Inverted colloidal crystal scaffolds based on biodegradable polyesters for cartilage tissue engineering: Production, physico-chemical characterization, and in vitro evaluation

Maike Coelho Afonso Gomes[a]

[a]MSc student in Biomedical Engineering, nº72460, UTL-IST
Under Supervision of Professor Cláudia Lobato da Silva and Professor Jorge Silva
Tissue Engineering Group, FCT-UNL, Lisbon, Portugal
June 2014

Abstract - Inverted Colloidal Cristal (ICC) scaffolds have been suggested by several groups due to their long-range ordered structure, well controlled pore sizes and high interconnectivity between pores. This unique hierarchical porosity facilitates the migration of cells and an efficient nutrient and oxygen diffusion along the entire structure.
In this study, polycaprolactone (PCL) ICC scaffolds with different pores sizes and polymer concentration were developed. To accomplish that, gelatin/poly(vinyl alcohol) (PVA) microspheres with 230, 280 and 340 µm diameter were produced and packed into a cubic close packed (ccp) lattice. In order to induce the necking between microspheres, a polyvinylpyrrolidone (PVP) solution was poured over the packed microspheres, turning this assembled structure into a solid colloidal crystal (CC). After impregnating this solid structure with PCL solution and subsequently freeze drying it, microspheres were dissolved and porous scaffolds with the inverted colloidal crystal (ICC) geometry were obtained.
To study the influence of pore sizes and polymer concentration on ICC's mechanical properties, ICCs were mechanically tested in compression. The lowest and the highest Young's modulus values obtained for the different ICC scaffolds were 0.84 MPa (280 µm pore and 20 % PCL) and 1.59 (280 µm pore and 40 % PCL), respectively. For in vitro evaluation, ICC scaffolds were seeded with ATDC5 cells. This cell line exhibits the multistep chondrogenic differentiation observed during endochondral bone formation. Adhesion rates around 30 % were obtain for both ICC types. Equal proliferation rates were verified for all ICC types during 11 days. Images of ATDC5 cells distributed along the entire ICC surface were obtained by staining cells with a blue fluorescent nucleic acid stain (DAPI). Glycosaminoglycans (GAGs) secreted by ATDC5 cells were visualized by staining ICC saffollds with Alcian Blue and Safranin-O on the 20th day after seeding.
Overall, the ordered pores of ICC constructs are a promising material for cartilage tissue engineering.

Keywords – Inverted Colloidal Cristal Scaffolds, Colloidal Cristal, Cartilage Tissue Engineering, Microspheres, ATDC5 cells

1. INTRODUCTION

Cartilage is an aneural and avascular flexible connective tissue composed of a specialized type of cells called chondrocytes embedded within a complex extracellular matrix consisting primarily of water, collagen, proteoglycans, glycosaminoglycans and non-collagenous proteins [1] [2].
It is the different biochemical composition and arrangement of this highly specialized structure that gives cartilage the capability to perform many functions in different tissues and parts of the body [3].In joints, articular cartilage is responsible to provide a deformable, low friction surface that enables the movement of articulating bones as well as the capacity to support high dynamic compressive loads [4]. Unfortunately, natural cartilage repair is limited, exhibiting a deficient self-recovery ability due to its avascular, alymphatic and nearly nonimmunogenic properties [5] [6] [7]. Thus, even minor injury may give rise to progressive damage and consequent degeneration of cartilage [8]. Osteoarthritis is a degenerative joint disease characterized by progressive degeneration of the articular cartilage, subchondral bone, menisci and sinovium, causing debilitating joint pain and stiffness that worsens over time. It is estimated that 27 million Americans suffer from OA, being more common in the elderly population [9] [10]. In a study performed in 2011, the prevalence of knee and hip osteoarthritis in Portugal were 11.1% and 5.5%, respectively [11]
Current clinical treatment strategies like microfracture, mosaicplasty and autologous chondrocytes injection have different success rates, however, average long-term results are

unsatisfactory [5]. To overcome these limitations, cartilage tissue engineering is an emerging field that has shown numerous progressions. This branch of Biomedical Engineering broadly involves the combinations of three components: cells, biological signal molecules and scaffolds [12].

Scaffolds are a key component for cartilage tissue engineering, consisting in a 3-dimensional structure that acts as a template for cell attachment, migration, proliferation, differentiation and synthesis of ECM while also providing a mechanically stable support until the new cartilage is formed [12] [5]. A plethora of fabrications technologies have been applied to develop 3D scaffolds for tissue engineering applications, namely solvent casting and particulate leaching, gas foaming, emulsion freeze drying, fiber bonding, electrospining, 3D printing and others. [13] [14]

Each of these manufacturing processes exhibits potential and limitations, however, most of these methods fail in one or more requirements like irregular pore size, poor interconnectivity, irregular structure and low mechanical properties [13] [15]

In order to overcome these limitations, 3D scaffolds based on inverted colloidal crystal (ICC) geometry have been suggested by several groups since they possess a long range ordered structure, well controlled pore sizes and uniform interconnections [16] The high interconnectivity of these inverse opal scaffolds facilitates the migration of cells and an efficient nutrient, waste and oxygen diffusion along the entire structure. To date, ICCs have been applied in a wide range of applications namely neovascularization, bone, liver, cartilage and neural tissue engineering [17]. ICC scaffolds are typically made in five step processes: i) production of uniform microspheres, ii) packaging of these microspheres into a cubic close packed (ccp) lattice, iii) thermal treatment (annealing) or other process to induce necking between adjacent microspheres, iv) filling the interstitial space with the scaffolding material and subsequent freeze-drying and v) dissolution of the microspheres, leaving an inverse opal structure behind

In this study, polycaprolactone (PCL) ICC scaffolds with different pores sizes and polymer concentration were developed, following all the five steps above mentioned. ICCs were mechanically tested in compression in order to study their mechanical properties.

For vitro evaluation, ICC scaffolds were seeded with ATDC5 cells. Adhesion rate, proliferation, cell distribution and glycosaminoglycans (GAGs) secretion were analyzed during 20 days of culture.

2. MATERIAL AND METHODS

2.1 Microspheres production

Gelatin (Gelatin from porcine skin; Sigma-Aldrich®) and Gelatin/Polyvinyl alcohol (Acros Organics) microspheres were produced by microfluidic technique. For the continuous phase, liquid paraffin (viscosity at 40ºC ≈ 72.6 cSt, Labchem) with 6% w/w sorbitan oleate (Fagron) contained in a 50 ml syringe (Omnifix®) was injected by an infusion pump (Baxter Flo-Gard GSP) into a teflon tube through a 17G needle. In order to form W/O droplets, the discontinuous phase contained in a 20 mL syringe (Omnifix®) was also injected through a 23G needle, which was inserted inside another teflon tube

For gelatin microspheres production, aqueous solutions with 5, 10 and 15 % w/w gelatin were used. For gelatin/PVA microspheres, a 10 % w/w gelatin aqueous solution with 1.5, 2.0 and 2.5% w/w PVA was used. Microsphere diameter was controlled through the variation of continuous and discontinuous phase flow rates, as well as gelatin concentration

After production, microspheres were frozen, allowing the aqueous phase droplets to gel quickly. Then, microspheres were washed with successive acetone/water solutions with a volume ratio of 4:3, 4:2, 4:1 and lastly only acetone. These procedure allowed the slow dehydration of the microspheres. Microspheres morphological analysis was done by optical microscope. 50 random samples of each production cycle were used to measure microspheres diameter with the help of ImageJ™

2.2. Microspheres Packing

For microspheres with an average diameter of 340, 280 and 230 µm, sieves with 355 and 300 µm, 250 and 280 µm and 250 and 212 µm, respectively, were used.

A mold consisting of 32 wells with 6mm diameter and 2mm height was developed for CC production. Isopropanol suspension of microspheres was slowly dropped to the wells and gently agitated by an orbital shaker (SK-330-Pro) in order to organize them into a hexagonal close-packed geometry. When the wells were full, the mold was left on the orbital shaker a further 45 minutes for isopropanol evaporation.

2.3. Annealing

A 5% polyvinylpyrrolidone (PVP, Sigma-Aldrich®) solution in isopropanol was poured over the packed microspheres. After isopropanol evaporation, PVP acts as a kind of glue that allows connectivity between

microspheres, turning the assembled structure into a linked solid construct.

2.4. CC impregnation

Solid CC was impregnated with a Polycaprolactone (Mw ≈ 43,000 – 50,000; Polysciences) solution in dioxane ($C_4H_8O_2$; Panreac). CC's of 230 and 340 µm microspheres were impregnated with 30% PCL solution, whereas CC's of 270 µm were impregnated with 20, 30 and 40% PCL solutions.
To carry out impregnations, CC's were immersed in the PCL solutions and subsequently put in a vacuum desiccator. The air removal by vacuum pump allowed PCL solution fill the interstitial spaces between microspheres. This process was repeated until no air bubbles were released from CC structure. Finally, CC's were frozen and posteriorly lyophilized in a freeze-drier (Vaco 2, Zirbus) during 24 hours

2.5. Inverted Colloidal Cristal (ICC) scaffold

After lyophilisation, the impregnated CCs were immersed in warm water at approximately 48 ºC, allowing the dissolution of the gelatin microspheres. Then, a PCL ICC scaffold was obtained.

2.6. Scanning electronmicroscopy (SEM)

CC's and ICC scaffolds were analyzed by SEM (*Zeiss DSM-962).*.

2.7. Mechanical Properties – Compression tests

In order to study mechanical properties, ICC scaffolds were mechanically tested in compression (*Rheometric Scientific equipment;* Minimat Firmware 3.1) using a 20 N load cell and a velocity of 0.2 mm/min. For each ICC type, 10 samples were used. From the force and compression values given by compression test, the stress vs. strain curves were plotted and the Young's modulus calculated.

2.8. Cell culture

2.8.1. ATDC5 Cells

In vitro studies were performed using ATDC5 cells. This cell line is derived from mouse teratocarcinoma cells and exhibits a multistep process of chondrogenic differentiation analogous to that observed during endochondral bone formation. Culture medium consisted in a 1:1 mixture of Dulbecco's modified Eagle's medium (DMEM) (Sigma-Aldrich) and HAM's F12 (Sigma-Aldrich) containing 5% Fetal Bovine Serum (FBS) (Invitrogen) and 1% antibiotic (penicillin-streptomycin, Invitrogen).

2.8.2. ICC scaffold preparation

Before sowing ATDC5 cells, 10 ICC scaffolds of each type (5 different types) were placed in a 96 well plate (each well with one ICC) and sterilized with ethanol 70 %. To avoid the floating of the scaffolds, air present into the structure was removed by a vacuum pump. After sterilization, ethanol was removed and ICC's were washed three tims with a phosphate buffered saline solution (PBS) (Invitrogen), and finally, with culture medium. Control ICC's (ICC's without cells) were prepared in the same way

2.8.3. ATDC5 cell culture

ATDC5 cells were seeded with a concentration of $7x10^3$ cells/well. To accomplish that, 100 µl of cell suspension was gently pipetted onto the ICC scaffold surface. After that, the 96 well plate was kept in a CO_2 incubator with the medium being changed every second day. From the second day on, the culture medium was substituted for DMEM:F12 with 100 µg/ml of ascorbic acid (L-Ascorbic acid 2- phosphate sesquimagnesium salt hydrate, Sigma-Aldrich) in order to induce ATDC5 cells differentiation. Control ICC's were treated in the same way, but without cells.

.

2.9. Resazurin assay

The resazurin assay is a simple, rapid and sensitive method to measure metabolic activity of living cells by the reduction of the non-fluorescent dye resazurin (blue) to the strongly-fluorescent dye resorufin (red). The amount of dye conversion can be measured spectrophotometrically. The resazurin solution was prepared by dissolving the powder (Alfa Aesar) in PBS at a concentration of 0.25 mg/ml. Following the removal of culture medium, 100µl of DMEM:F12 with 10% resazurin solution was pipetted into each well. The 96 well plate was kept in the CO_2 incubator at 37ºC during 3 hours for the reaction to occur. After 3 hours, 90 µl of each well was pipetted to another 96 well plate, which is posteriorly placed in a spectrophotometer (ELX800 Biotek) to read A_{570} and A_{600}. After that, ICC's and cell controls were washed with PBS once to remove the remaining resazurin solution. Finally, 100 µl of medium was added to each well and the microplate was placed back in the incubator.

2.9.1. Adhesion rate

To calculate the adhesion rate, all ICC types were initially transferred to other 96 well plate. Then, the above mentioned procedure was done for ICC's present in the new plate, for the wells where ICC's were initially (to count how many cells adhered to the well surface instead of to the scaffold), for cell controls and for both

medium controls. After absorbance reading, it was possible to calculate adhesion through simple equations showed in results.

2.9.2. Proliferation

In order to evaluate the proliferation of ATDC5 cell in ICC scaffolds, resazurin assay was performed every second day during 9 days.

2.10. DAPI Nucleic Acid Stain

In order to see the cell distribution along the ICC surface, ATDC5 cells were stained with DAPI (Invitrogen), which is blue fluorescent nucleic acid stain that preferentially stains dsDNA.
To prepare DAPI stock solution, 10 mg of DAPI was dissolved in 2 mL of deionized water. Posteriorly, this stock solution was diluted to 300nM in PBS. Initially, ICC's were rinsed once with PBS and fixed for 15 minutes at room temperature (RT) with 3,4% paraformaldehyde (PFA). After removal of PFA, ICC's were washed three times with PBS. 100 µl of DAPI solution was pipetted for each ICC and left to act during 5 minutes at RT. To finalize, ICC were washed 3 times with PBS, observed using fluorescence microscopy, and images taken

2.11. Chondrogenic differentiation staining

2.11.1 Alcian Blue Staining

To demonstrate chondrogenesis by identification of sulfated glycosaminoglycan deposits (synthetized by ATDC5 cells), the Alcian Blue staining method was used. Following the removal of the differentiation medium, ICCs were washed with PBS and fixed with 3,4 % PFA for 15 minutes at RT. After that, the PFA was removed and ICC's were washed three times with PBS. 100 µl of 1% Alcian Blue (Alfa Aesar) solution prepared in 3% acetic acid were pipetted to each ICC, and left to act during 10 minutes. ICC were rinsed 4 times with PBS in order to remove excess staining. To finalize, ICC's were left overnight at RT to dry and observed under optical microscope.

2.11.2. Safranin-O staining

To stain cells with safranin, 0.1 % safranin (Alfa Aesar) solution dissolved in deionized water was prepared. The staining protocol was the same as for Alcian Blue.

3. Results and Discussion

3.1. Gelatin microspheres production

Initially, an aqueous solution of 5% gelatin was pumped with a flow rate of 2 mL/h. Continuous phase consisting of liquid paraffin and sorbitan oleate (SPAN 80) was ejected with a flow rate of 10mL/h. The resulting W/O droplets were expelled from the teflon tube and collected in a large plastic recipient. After a few hours, water present in the droplets evaporates and solid microspheres are formed. Microspheres with smaller diameters were produced repeating the same procedure but now for 18 and 26 mL/h of flow rates.
In order to study the influence of gelatin concentration on microsphere size, all the aforementioned steps were repeated for 10 and 15 % gelatin aqueous solutions.
Due to the low polymer concentration, 5% gelatin microspheres, suffered a high shrinking during water evaporation, giving rise to a wrinkled appearance. When 10% and 15% gelatin aqueous solution is used, microspheres present a more rounded shape and smooth surface. As continuous phase flow rate increases, microspheres diameter decreases, as expected. When gelatin concentration is increased and flow rates are kept, microspheres diameter increases.
After observing microspheres by optical microscope, it was visualized that many of them had a flattened shape, as can be seen in figure 1.This outcome is due to the drying process. When water slowly evaporates, the gelatin network shrinks and collapses, depositing itself on the surface where it is supported, and so, a flattened morphology is obtained.

Figure 1 - Flattened gelatin microspheres.

To avoid this situation, glutaraldehyde was used as a crosslinking agent to obtain rigid microspheres. Microspheres with a perfect spherical shape were obtained through this method (figure 2). However, these microspheres became insoluble due to crosslinking, being impossible to dissolve them afterwards. This is a huge problem since it is necessary to remove microspheres from the ICC scaffolds
Since microspheres dried by slow evaporation have a flattened shape and the use of glutaraldehyde prevents their dissolution, another method to dry the microspheres was attempted. Briefly, gelatin microspheres are placed in a refrigerator to allow the aqueous

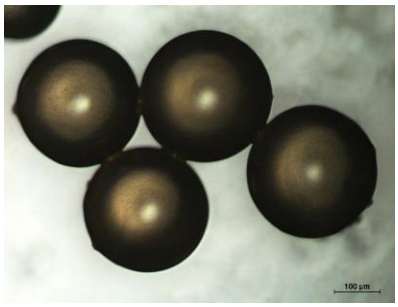

Figure 2 - Gelatin microspheres cross-linked with glutaraldehyde.

phase droplets to gel quickly and then rinsed with successive acetone/ water solutions with a volume ratio of 4:3, 4:2, 4:1 and lastly only acetone. To achieve complete dehydration, microspheres are then put in isopropanol. This procedure enables the removal of water in a slowly and gently way. Despite microspheres resulted from this dried process present a more spherical shape comparatively to microspheres dried by slow water evaporation, some of them present defects.

3.2. Gelatin/PVA microspheres production

To overcome this problem, polyvinyl alcohol (PVA) was added in order to stabilize the emulsion between gelatin aqueous solution and paraffin. The hydroxyl groups in PVA interact with the water phase while the vinyl chain interact with the paraffin thus making the formed emulsion more stable. To study the effect of PVA concentration on microsphere shape, 10 % gelatin aqueous solution with 1.5, 2.0 and 2.5 % of PVA were prepared.

For all concentrations, it was evident the effect of PVA in microspheres morphology, presenting a more spherical shape comparatively to the previously obtained**.**

With PVA addition, the solutions become more viscous and, subsequently, W/O droplets are formed in jetting mode instead of dripping mode As a result, the droplets have a larger range in size, and consequently microspheres have a larger size distribution. Since gelatin solution with 2.5 % of PVA is very viscous, it was decided to use 10 % gelation aqueous solution with 2% PVA to produce the final microspheres. Using a discontinuous flow rate of 1,5 mL/h, microspheres around 340, 280 and 230 µm were obtained with 30, 35 and 40 mL/h continuous flow rates, respectively (table 1). These were the sizes chosen to develop the ICC scaffolds.

Table 1 - Production of 10 % gelatin microspheres with 2% PVA. CF-continuous phase, DF discontinuous phase.

CF (mL/h)	DF(mL/h)	Diameter (µm)	Standard deviation (µm)
25	1,5	385	26
30		338	28
35		281	27
40		234	29

3.3. Microspheres packaging and annealing

After separate the microspheres with different sieves, the isopropanol suspension of microspheres was slowly dropped to the mold and gently agitated by an orbital shaker. Thus, a hexagonal close-packed geometry was obtained.

In order to induce the necking between microspheres, a 5% PVP solution in isopropanol was used. After isopropanol evaporation, PVP acts as a kind of glue that allows connectivity between microspheres.

However, it was observed that a PVP film is formed between microspheres at the top of the well (the last microspheres layer to be formed is more exposed to air). When the CC is impregnated, this film does not allow the polymer solution to occupy the spaces between microspheres, giving rise to an irregular surface.

3.4. Colloidal Cristals (CCs)

CCs with microspheres of 230, 280 and 340 µm were visualized by scanning electron microscopy (SEM). As the microspheres size increase, they tend loose their spherical shape and present a rougher surface. The small differences in diameter are enough to change all the organization, which will compromise the interconnection between pores. Several contact sites between microspheres are missing and so, these flaws will slightly increase the void volume in the particle array.

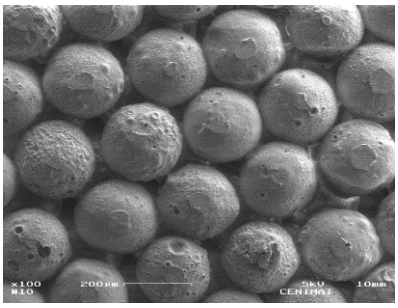

Figure 3 - SEM images of CC's with 280 µm microspheres

3.5. Inverted Colloidal Cristals (ICCs)

After obtaining a solid CC, this structure was impregnated with the polymer solution. To study the effect of the polymer concentration during cell culture as well as the mechanical properties of the ICC's scaffolds, CC's with microspheres of 230 and 340 µm were impregnated with 30% PCL solution, whereas CC's of 280 µm were impregnated with 20, 30 and 40% PCL solutions.

After freezing and freeze drying the impregnated CCs, gelatin microspheres were selectively removed by immersing the samples in a water bath heated at 48 ºC, giving rise to PCL ICC scaffold.

As can be seen in figure 4 it is extremely difficult to have a perfectly close packed array due to the non-uniform sizes and shapes of microspheres. Due to the absence of contact sites between microspheres, not all the cavities present the three interconnecting channels between them, as expected. Consequently, the transport of nutrients and oxygen to the inside of the scaffolds as well as cell migration will be compromised.

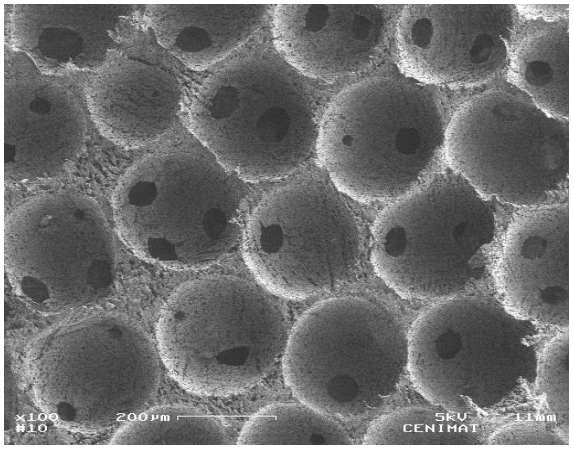

Figure 4 – SEM images of an ICC scaffold with pores of 280 µm and 30% PCL.

In general, as the pore size increase, the interconnection channels between pores also increase.

After measuring the intercavity pore from the SEM images, ICC scaffolds of 230, 280 and 340 µm presented interconnecting pores of approximately (38 ± 9) µm, (56 ± 11) µm and (68 ± 14) µm, respectively.

The intercavity pore depends mainly in the contact between microspheres and by the bridge created by PVP.

In order to evaluate the influence of polymer concentration on the ICCs microstructure, ICCs produced from solutions with 20, 30 and 40% PCL were visualized in SEM. As the polymer concentration decreases, the structure resulting from the freeze-drying process becomes more porous (figure 5). These differences in porosity also influence the mechanical properties of ICC scaffolds. PCL solutions with higher concentrations are more viscous, and therefore it is more difficult to impregnate them. As a consequence, there is a higher probability of distorting the particle array due the infiltration stress, comparatively with lower concentration solutions.

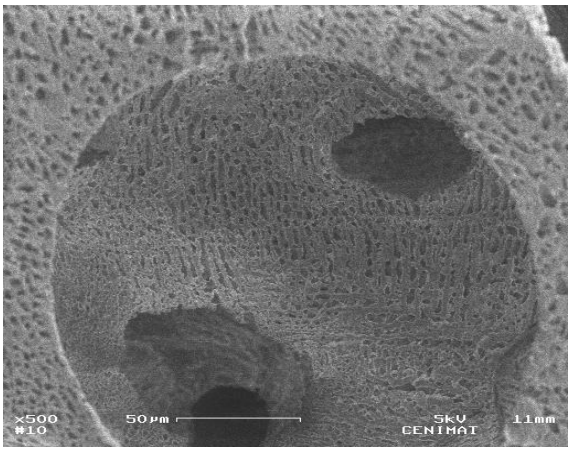

Figure 5 - SEM images of an ICC scaffold with 280 µm pores and 20 % PCL.

3.6. Mechanical properties

In order to study the mechanical properties, ICC scaffolds were mechanically tested in compression. During this assay, a compression force perpendicular to the material surface was applied, resulting in a progressive deformation of the structure. The resistance that the ICC scaffold offers to the applied stress depends of the porosity and polymer density. From the force and compression values given by compression test, it is possible to plot the stress vs. strain curves (figure 6), and therefore, calculate the Young modulus by the linear region slope.

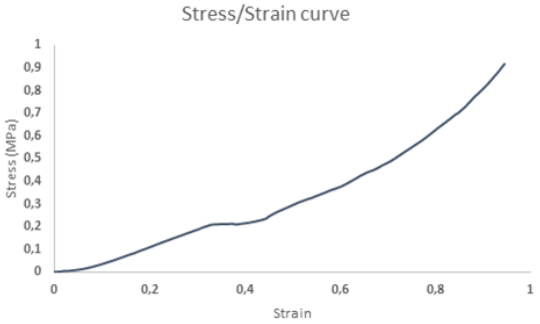

Figure 6 - Stress-strain curve of an ICC scaffold with 230 µm pores and 20% PCL.

When ICC scaffold have the same pore sizes and PCL concentration is increased, Young's modulus also increases, as expected. On the other hand, when ICC's have the same PCL concentration and pore sizes increase, Young's modulus decrease slightly. Since microspheres with larger sizes tend to lose their spherical shape, the CC organization will be more affected and consequently, ICCs have smaller Young's modulus values.
The smaller Young's modulus values was obtained with 280 µm pore sizes and 20 % PCL, with an average of 0.84 MPa, whereas the higher Young modulus was obtained with 280 µm pore sizes and 40% PCL, with an average of 1.59 MPa.
In order to evaluate if these values are acceptable, they were compared with other PCL scaffolds with interconnected spherical porous [18] The elastic modulus values of these PCL scaffolds with different porosities are listed in table 2.

Table 2 - Young modulus of PCL scaffolds with different porosities [18].

Porosity	74.6 ±1.6	80.1 ±1.6	85.9 ±2.4
E (MPa)	2.57±0.99	1.82±0.16	0.6 ±0.12

Considering an ICC scaffold with 280 µm pore size and 40 % PCL, the porosity will be approximately 89,6% (hexagonally arrayed microspheres occupied about 74% of the lattice volume in theory). Of course, due the non-uniform sizes and shapes of microspheres, the porosity is slightly smaller.
Observing the Young's modulus present in gray columns, it can be concluded that the results obtained are consistent with reported literature values. The rigidity value interval reported for human articular cartilage is between 0.51 and 1.82 MPa [18]. Since all the Young's modulus obtained lie in this interval, ICC scaffolds are an interesting candidate for cartilage engineering, at least from the mechanical point of view.

3.7. In vitro studies

3.7.1. Adhesion rate

In order to calculate the adhesion rate through resazurin assay, A_{570} and A_{600} were first measured.
After obtain the absorbance results of the ICC's, the wells where ICC's were initially (SICC) and the cell controls (CC), the medium contribution was subtracted through the following equations:

$$X(A_{570} - A_{600})_{ICC} - X(A_{570} - A_{600})_{ICCMC} \quad 1$$

$$X(A_{570} - A_{600})_{SICC} - X(A_{570} - A_{600})_{MC} \quad 2$$

$$X(A_{570} - A_{600})_{CC} - X(A_{570} - A_{600})_{MC} \quad 3$$

Where X, MC and ICCM represents the average, the medium control and the medium control for ICCs (ICCs without cells), respectively.
Finaly, adhesion rate (AR) can be calculated by:

$$\frac{\text{RESULT EQ 1}}{(\text{RESULT EQ 3} - \text{RESULT EQ 2})} \quad 4$$

Adhesion rates around 20 % were obtained for both ICC's, which are somewhat low values. In order to analyze these results, a study to understand how resazurin concentration influences the absorbance results was performed. It was seen that when resazurin concentrations are duplicated, the conversion of resazurin to resarufin also duplicates, using the same number of cells and incubating time. Before adding the 10 % resazurin solution, the medium culture of ICC's needs to be aspirated. Since ICC scaffolds are porous, the culture medium occupies these spaces, being extremely difficult aspirate all the medium. Thus, the medium present within ICC's will dilute the 10% resazurin solution, influencing the final results. To know the amount of medium that remains in ICC's after aspiration, ICC's were weighted with and without medium. On average, 40 µl remains within each ICC scaffold. Since 100ul of 10% resazurin solution are added to each ICC, resazurin concentration decreases to 7.14 % and, subsequently, the true adhesion rates would be approximately 30%.
In order to increase the adhesion rates, ICC scaffold surfaces should be chemically modified to promote cell attachment. A simple way to do that is based in a sodium hydroxide (NaOH) treatment which creates surface nanotopography with improved hydrophilicity.

3.7.2. ATDC5 cell proliferation

To study cell proliferation, the resazurin assay was performed every second day during 9 days. The blue rows in table 3 represent the result obtained by equation 1, whereas the white rows represent the standard deviation for each ICC type. As can be seen in table 3, ATDC5 cells proliferated over time. No significant differences were obtained among the five different ICC scaffolds. Between day 1 and 3, the highest proliferation rate was recorded.

Table 3 - ATDC5 cells proliferation

		230 µm 30% PCL	270 µm 20% PCL	270 µm 30% PCL	270 µm 40% PCL	330 µm 30% PCL	Cell Control
Day 1	**Absorbance**	0,084	0,071	0,073	0,079	0,082	0,519
	Standard deviation	0,014	0,007	0,004	0,009	0,011	0,016
Day 3	**Absorbance**	0,287	0,263	0,268	0,295	0,285	0,821
	Standard deviation	0,052	0,039	0,029	0,038	0,029	0,046
Day 5	**Absorbance**	0,644	0,605	0,624	0,631	0,649	1,283
	Standard deviation	0,081	0,955	0,088	0,080	0,051	0,038
Day 7	**Absorbance**	0,802	0,807	0,776	0,753	0,789	1,431
	Standard deviation	0,069	0,073	0,101	0,071	0,046	0,035
Day 9	**Absorbance**	0,922	0,966	0,903	0,851	0,880	1,515
	Standard deviation	0,067	0,039	0,071	0,072	0,051	0,028

At day 9, ICC scaffolds had approximately 60% of cells present in controls. In order to know if cells can migrate to the entire structure, and thus have more space to proliferate than the controls in the 96 well plate, resazurin assay should be done during more days until the number of cells were higher than control.

3.8. DAPI nuclei acid stain

DAPI is a blue fluorescent nucleic acid stain that stains preferentially double-stranded DNA (dsDNA). The fluorescence is directly proportional to the amount of DNA present, with a maximum emission at ~460nm.
ICC scaffolds were stained with DAPI in order to observe the cell distribution along the entire surface.
ATDC5 cell nucleus were well stained with DAPI, being broadly distributed throughout the ICC scaffold.
Figure 7 was edited to enhance contrast and give a better understanding of the distribution of cells. No significant differences were obtained between each ICC type

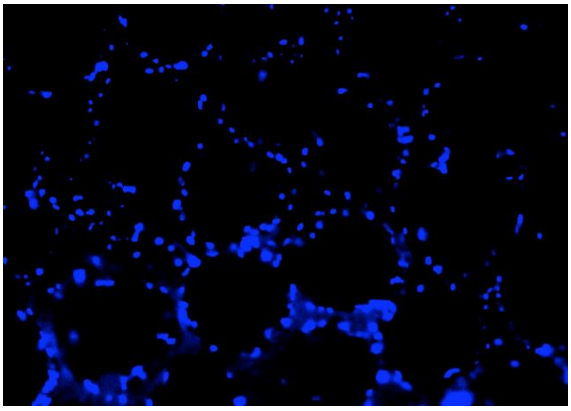

Figure 7 - ICC with 330 µm pores and 30% PCL stained with DAPI.

3.9. Chondrogenic differentiation staining

In order to evaluate the chondrogenic capacity of ATDC5 cells, ICCs were stained with Alcian Blue and Safranin-O on the 20th day after the sowing, and posteriorly visualized using optical microscopy. As can be seen in figure 8 and 9, ICC scaffolds present small blue (Alcian Blue) and orange-red (Safranin) stains within the pores cavity, which can prove the presence of GAGs secreted by ATDC5 cells.
In order to know if the blue stains observed are really due to the presence of GAGs and not just by the absorption capacity of PCL, the staining protocol was repeated for ICCs without cells.
ICC controls do not present these strong blue stains comparatively with the others, confirming the presence of GAGs. We did not observe a significant difference between ICC types, being difficult to understand if polymer concentration

and pore sizes have any influence on GAGs secretion.
However, from these results it can only be concluded that there is secretion of GAGs on the ICC surfaces. To know if the chondrogenesis occurred along the entire structure, it would be necessary to slice the ICC scaffolds, for instance, by a cryostat microtome, and perform histological staining. From this procedure, it would be possible to see if ATDC5 cells migrated along the entire ICC scaffold.

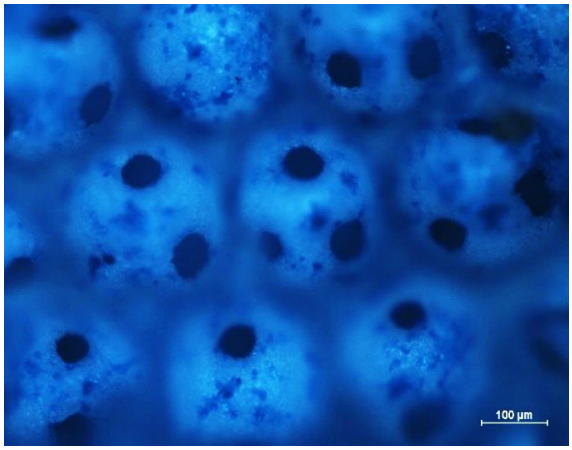

Figure 8 - ICC with 280 µm pores and 30 % PCL stained with Alcian Blue on the 20th day after seeding. **Scale bar =** 100 µm

Figure 9 - ICC with 280 µm pores and 30 % PCL stained with Safranin on the 20th day after seeding. **Scale bar =** 100 µm

3.10. RT-PCR

In order to evaluate the expression of collagen II, we tried to perform RT-PCR for the different ICC scaffolds. Initially, cells were detached from scaffolds using trypsin. However, after counting the number of retrieved cells, a too small number was obtained. In order to overcome this problem, the RNA was isolated directly from ICC scaffolds, applying the lysis solution on these structures. After following the protocol (High Pure RNA Isolation Kit, Roche), the RNA concentration was quantified, obtaining a low concentration (≈10 ng/µl) comparatively to the minimum required to convert RNA to cDNA (≈100 ng/µl). Thus, it was not possible to study the expression of this chondrogenic marker.
One way to enhance the RNA yield would be to increase the initial cell concentration. However, if there is a high cell density, cells tend to stack on top of each other, and consequently, the real influence of the scaffold is not evaluated. Other simple and useful method to improve RNA yield would be the increase of the centrifugation times along the entire RNA extraction protocol.´

4. Conclusion and future work

The long-range well-ordered structure, uniform pore size and regular 3D interconnectivity of ICC scaffolds make them suitable for the most challenging tasks in tissue engineering.
In this work, PCL ICC scaffolds with different pore sizes and polymer concentration were developed.
Gelatin microspheres with different sizes were produced by the microfluidic technique. However, it was observed that many of these microspheres presented a flattened morphology due to the drying process (slow evaporation).
To overcome this drawback, polyvinyl alcohol (PVA) was added to gelatin microspheres in order to stabilize the emulsion between gelatin aqueous solution and paraffin. The effect of this emulsifier on microspheres morphology was evident, presenting a more spherical shape comparatively to the previously obtained.
SEM images of ICCs demonstrated that it is extremely difficult to have a perfectly close packed array due to the non-uniform sizes and shapes of microspheres. Even the small differences in microspheres diameter are enough to affect all the organization, compromising the interconnection between pores
From the mechanical point of view, ICCs seems to be an interesting candidate for cartilage tissue engineering, since their Young's modulus lie in the rigidity value interval reported for human articular cartilage (between 0.51 and 1.82 MPa).
Relatively to in vitro evaluation, the values obtained for the adhesion rates were slightly low. In order to increase these values, ICC scaffold surfaces should be chemically modified to promote cell attachment.
At day 9, ICC scaffolds had approximately 60% of cells present in controls. After a certain time, the number of cells present in ICCs will probably exceed the control, since they have more space to proliferate. This outcome will be influenced

mainly by the well-ordered structure and 3D interconnectivity of ICC scaffold. If there are no interconnections between pores, cells cannot migrate to occupy all the scaffold spaces, and consequently, proliferation will cease

GAGs secretion was proved by Alcian Blue and Safranin-O staining on the 20th day after the sowing. Small blue (Alcian Blue) and orange-red (Safranin) stains within the pores were observed, which prove the presence of GAGs secreted by ATDC5 cells.

During the entire work, it was difficult to understand if polymer concentration and pore sizes influences de proliferation and differentiation of ATDC5 cells. An evaluation of chondrogenic marker expression such as collagen II, SOX 9 and Runx2 would be important to really understand the influence of these two characteristics. Despite the high potential of ICC scaffolds, it is extremely difficult to have a long range ordered structure, with controlled pore sizes and uniform interconnections.

Microspheres with uniform sizes and perfectly spherical shape are crucial for the development of ideal ICC scaffolds. If one of these feature fails, all organization will be compromised. More work needs to be done in order to improve all the steps necessary for the development of an ICC scaffold. All of them, without exception, are essential to obtain a perfect structure.

REFERENCES

1. Sharma, C., et al., *Cartilage tissue engineering: current scenario and challenges.* Adv. Mat. Lett, 2011. 2(2): p. 90-99.
2. Milner, P.I., R.J. Wilkins, and J.S. Gibson, *Cellular Physiology of Articular Cartilage in Health and Disease. 2012*
3. Wachsmuth, L., et al., *Immunolocalization of matrix proteins in different human cartilage subtypes.* Histol Histopathol, 2006. 21(5): p. 477-85.
4. Izadifar, Z., X. Chen, and W. Kulyk, *Strategic Design and Fabrication of Engineered Scaffolds for Articular Cartilage Repair.* Journal of Functional Biomaterials, 2012. 3(4): p. 799-838.
5. Kock, L., C.C. van Donkelaar, and K. Ito, *Tissue engineering of functional articular cartilage: the current status.* Cell Tissue Res, 2012. 347(3): p. 613-27.
6. Kuo, Y.C. and Y.T. Tsai, *Inverted colloidal crystal scaffolds for uniform cartilage regeneration.* Biomacromolecules, 2010. 11(3): p. 731-9.
7. Omata, S., Y. Sawae, and T. Murakami, *Tissue Development and Mechanical Property in the Regenerated-Cartilage Tissue.* 2012.
8. Johnstone, B., et al., *Tissue engineering for articular cartilage repair--the state of the art.* Eur Cell Mater, 2013. 25: p. 248-67.
9. Van Liew, C., et al., *The Good Life: Assessing the Relative Importance of Physical, Psychological, and Self-Efficacy Statuses on Quality of Well-Being in Osteoarthritis Patients.* Arthritis, 2013.
10. Rezende, M.U.d., G.C.d. Campos, and A.F. Pailo, *Current concepts in osteoarthritis.* Acta ortopedica brasileira, 2013. 21(2): p. 120-122.
11. Monjardino, T., R. Lucas, and H. Barros, *Frequency of rheumatic diseases in Portugal: a systematic review.* Acta Reumatológica Portuguesa, 2011. 36(4).
12. Mollon, B., et al., *The clinical status of cartilage tissue regeneration in humans.* Osteoarthritis and cartilage / OARS, Osteoarthritis Research Society, 2013. 21(12): p. 1824-1833.
13. João, C.F., et al., *An overview of inverted colloidal crystal systems for tissue engineering.* Tissue Engineering, 2013.
14. Draghi, L., et al., *Microspheres leaching for scaffold porosity control.* Journal of materials science: materials in medicine, 2005. 16(12): p. 1093-1097.
15. Koch, T.G., et al., *Joint Cartilage Tissue Engineering and Pre-Clinical Safety and Efficacy Testing.*
16. Zhang, Y.S., K.P. Regan, and Y. Xia, *Controlling the pore sizes and related properties of inverse opal scaffolds for tissue engineering applications.* Macromolecular rapid communications, 2013. 34(6): p. 485-491.

17. Zhang, Y.S., et al., *Fabrication of cell patches using biodegradable scaffolds with a hexagonal array of interconnected pores (SHAIPs).* Polymer, 2014. 55(1): p. 445-452.
18. Lebourg, M., et al., *Biodegradable polycaprolactone scaffold with controlled porosity obtained by modified particle-leaching technique.* Journal of Materials Science: Materials in Medicine, 2008. 19(5): p. 2047-2053.